Neuron, Vol. 17, 1005–1013, November, 1996, Copyright ©1996 by Cell Press

Familial Alzheimer's Disease–Linked Presenilin 1 Variants Elevate Aβ1–42/1–40 Ratio In Vitro and In Vivo

David R. Borchelt,[1,4,11] Gopal Thinakaran,[1,4,11] Christopher B. Eckman,[5,6,11] Michael K. Lee,[1,4,11] Frances Davenport,[4] Tamara Ratovitsky,[4] Cristian-Mihail Prada,[6] Grace Kim,[4] Sophia Seekins,[4] Debra Yager,[6] Hilda H. Slunt,[4] Rong Wang,[7] Mary Seeger,[8] Allan I. Levey,[9] Samuel E. Gandy,[8] Neal G. Copeland,[10] Nancy A. Jenkins,[10] Donald L. Price,[1,2,3,4] Steven G. Younkin,[5,6] and Sangram S. Sisodia,[1,2,4]

[1]Department of Pathology
[2]Department of Neuroscience
[3]Department of Neurology
[4]Neuropathology Laboratory
The Johns Hopkins University
School of Medicine
Baltimore, Maryland 21205
[5]Department of Neuroscience
Case Western Reserve University
Cleveland, Ohio 44106
[6]Mayo Clinic Jacksonville
Jacksonville, Florida 32224
[7]Mass Spectrometry Laboratory
The Rockefeller University
New York, New York 10021
[8]Department of Neurology and Neuroscience
Cornell University Medical College
New York, New York 10021
[9]Department of Neurology
Emory University School of Medicine
Atlanta, Georgia 30322
[10]Mammalian Genetics Laboratory
ABL-Basic Research Program
NCI-Frederick Cancer Research and Development
Frederick, Maryland 21702

Summary

Mutations in the presenilin 1 (PS1) and presenilin 2 genes cosegregate with the majority of early-onset familial Alzheimer's disease (FAD) pedigrees. We now document that the Aβ1–42(43)/Aβ1–40 ratio in the conditioned media of independent N2a cell lines expressing three FAD-linked PS1 variants is uniformly elevated relative to cells expressing similar levels of wild-type PS1. Similarly, the Aβ1–42(43)/Aβ1–40 ratio is elevated in the brains of young transgenic animals coexpressing a chimeric amyloid precursor protein (APP) and an FAD-linked PS1 variant compared with brains of transgenic mice expressing APP alone or transgenic mice coexpressing wild-type human PS1 and APP. These studies provide compelling support for the view that one mechanism by which these mutant PS1 cause AD is by increasing the extracellular concentration of Aβ peptides terminating at 42(43), species that foster Aβ deposition.

[11] These authors contributed equally to this work.

Introduction

Alzheimer's disease (AD), a progressive neurodegenerative disorder, is associated with several risk factors, including age and inheritance. The majority of early-onset cases of AD are inherited as autosomal dominant disorders and cosegregate with mutations in the following: the presenilin 1 (*PS1*) gene on chromosome 14 (St George-Hyslop et al., 1992; Sherrington et al., 1995; Alzheimer's Disease Collaborative Group, 1995; Wasco et al., 1995; Campion et al., 1995; Chapman et al., 1995; Cruts et al., 1995; Boteva et al., 1996; Perez-Tur et al., 1995); the presenilin 2 (*PS2*) gene on chromosome 1 (Levy-Lahad et al., 1995a, 1995b; Rogaev et al., 1995); and the amyloid precursor protein (*APP*) gene on chromosome 21 (Goate et al., 1991; Chartier-Harlin et al., 1991; Naruse et al., 1991; Mullan et al., 1992; Hendriks et al., 1992). Mutations in *PS1* and *PS2* are causative in ~50% of pedigrees with early-onset FAD (Schellenberg, 1995).

The mechanism(s) by which FAD-linked mutations in *PS* cause AD have not been defined. However, recent studies indicate that conditioned medium from fibroblasts or plasma of affected members of pedigrees with *PS1/PS2*-linked mutations show a highly significant increase in the ratio of Aβ1–42(43)/Aβ1–40 relative to unaffected family members (Scheuner et al., 1996). The emerging view that Aβ1–42(43) plays a critical role in the pathogenesis of AD is supported by several lines of evidence as follows: first, physical chemical studies indicate that Aβ1–42(43) nucleates rapidly and is more fibrillogenic than Aβ1–40 (Burdick et al., 1992; Jarrett et al., 1993; Jarrett and Lansbury, 1993); second, several FAD-linked mutations in APP alter the processing of APP in cultured cells, leading to increased levels of Aβ1–42 in culture medium (either with or without increasing the levels of Aβ1–40) (Cai et al., 1993; Citron et al., 1992; Suzuki et al., 1994); third, Aβ1–42 is the principal component of amyloid deposits (Roher et al., 1993); and fourth, immunocytochemical and biochemical studies that document early and selective deposition of Aβ1–42(43) species in brains of patients with AD (Iwatsubo et al., 1994; Gravina et al., 1995) and Down's Syndrome (Iwatsubo et al., 1995; Lemere et al., 1996a). More recently, massive Aβ42(43) deposits were demonstrated in the cerebral cortex and cerebellum of individuals with a PS1-linked E280A mutation (Lemere et al., 1996b).

To examine directly the effects of wild-type and mutant PS1 on the ratio of Aβ peptide species, we quantified the levels of secreted Aβ1–42(43) and Aβ1–40 in the conditioned medium of stable mouse neuroblastoma (N2a) cell lines that constitutively express human APP in combination with wild-type PS1 or FAD-linked PS1 variants. We document that the ratios of Aβ1–42(43)/Aβ1–40 in media of independent cell lines expressing different FAD-linked PS1 variants (i.e., A246E, M146L, or ΔE9 variants) are uniformly elevated compared with the Aβ1–42(43)/Aβ1–40 ratios in media from cells that express essentially indistinguishable levels of wild-type PS1. We extended these analyses to examine whether

mutant PS1 influences Aβ1–42(43) production in the CNS. We mated transgenic mice expressing either human PS1 (Hu PS1) or Hu PS1 harboring an FAD-linked A246E mutation with transgenic mice expressing elevated levels of chimeric murine (Mo/Hu) APP-695 harboring a Hu Aβ domain and mutations (K595N, M596L) linked to Swedish FAD pedigrees (APPswe) (Mullan et al., 1992). We document that in the brains of young transgenic animals coexpressing APPswe and mutant PS1, the ratio of Aβ1–42(43) to Aβ1–40 is elevated as compared with transgenic mice expressing APPswe alone or transgenic mice coexpressing Hu PS1 and APPswe. Collectively, our studies of transfected cells and transgenic mice provide compelling support for the view that mutant presenilin acquires property(ies) that influence APP processing in a manner that results in elevated extracellular concentrations of Aβ1–42(43), a highly amyloidogenic peptide that is selectively deposited in the brains of individuals with AD and Down's Syndrome (Iwatsubo et al., 1994; Gravina et al., 1995; Lemere et al., 1996a).

Results

Expression of Human PS1 and APP in N2a Cell Lines

Stable mouse neuroblastoma (N2a) cell lines were generated that express the following: wild-type human APP alone (one line); human APP-695 with human wild-type PS1 (two lines); and human APP-695 with three different FAD-linked PS1 variants (M146L [four lines], PS1 A246E [two lines], and PS1ΔE9 [five lines]). The steady-state expression of APP and PS1 in each cell line was quantified by Western blotting, [^{125}I]protein A detection and phosphorimaging.

To examine PS1 expression, we used αPS1Loop, an antiserum that specifically reacts with epitopes in the hydrophilic "loop" domain of PS1 (amino acids 263–407) (Thinakaran et al., 1996). We recently reported that PS1 is subject to endoproteolytic processing in vivo, and the preponderant PS1-related species that normally accumulate in cultured mammalian cells, and in the brains of rodents, primates, and humans are ~27–28 kDa N-terminal and ~16–17 kDa C-terminal derivatives (Thinakaran et al., 1996). In untransfected N2a cells (data not shown) and N2a cells expressing human APP alone (Figure 1A, lane 1), αPS1Loop antiserum detected an ~16 kDa C-terminal PS1 derivative of mouse PS1. Moreover, and consistent with our earlier observations in African monkey kidney COS-1 and human embryonic kidney 293 cells expressing human PS1 (Thinakaran et al., 1996), αPS1Loop antiserum detected ~43 kDa and ~17 kDa polypeptides, corresponding to full-length human PS1 and a C-terminal human PS1 derivative, respectively, in N2a lines that stably coexpress human APP and human wild-type PS1 (Figure 1A, lanes 2 and 3). Both the full-length PS1 and ~17 kDa human PS1 derivative were detected in lines that stably coexpress the M146L (Figure 1A, lanes 4–7) or A246E (Figure 1A, lanes 8 and 9) PS1 variants. These results demonstrate that these FAD-linked PS1 variants are efficiently processed. In lines expressing the ΔE9 PS1 variant (Figure 1A, lanes 10–14), αPS1Loop detected variable levels of an ~40 kDa PS1 E9 polypeptide, a variant that is not a substrate for endoproteolysis (Thinakaran et al., 1996), and low levels of the ~16 kDa mouse PS1 derivative. Interestingly, the ~16 kDa endogenous mouse PS1 derivative failed to accumulate in cell lines expressing high levels of the M146L (line ML.10, Figure 1, lane 7), A246E (line AE.29, lane 9), or ΔE9 (line ΔE9.18, lane 14) variants. These results parallel our earlier demonstration that the mouse ~16 kDa PS1 derivative is undetectable in the brains of transgenic mice that overexpress human PS1 (Thinakaran et al., 1996), and appears to be replaced by the human ~17 kDa PS1 derivative.

In parallel, we examined the levels of N-terminal PS1, ~27–28 kDa derivatives in the N2a lines using Ab14, a polyclonal serum specific for amino acids 3–15 of human and mouse PS1 (Figure 1B). As expected, Ab14 detected an ~28 kDa N-terminal PS1 derivative in N2a cells expressing human APP alone (Figure 1B, lane 1) and ~43 kDa and ~27 kDa polypeptides, corresponding to full-length human PS1 and an N-terminal human PS1 derivative, respectively, in N2a lines stably expressing human wild-type PS1 (Figure 1B, lanes 2 and 3), M146L PS1 variant (Figure 1B, lanes 4–7), or A246E PS1 variant (Figure 1B, lanes 8 and 9, respectively). As expected, Ab14 detected the ~40 kDa PS1ΔE9 polypeptide in lines expressing the ΔE9 PS1 variant and the endogenous ~28 kDa N-terminal derivative (Figure 1B, lanes 10–14). In addition, the ~28 kDa mouse N-terminal PS1 derivative failed to accumulate in cell lines expressing high levels of the M146L (Figure 1, lane 7), A246E (lane 9), or the ΔE9 variant (lane 14), a result that mimicked the compromised accumulation of the mouse ~16 kDa C-terminal derivative in these lines.

To determine the steady-state levels of accumulated APP in stable N2a lines, we used antibody CT15, a polyclonal antiserum raised against the C-terminal 15 residues of APP (Sisodia et al., 1993). As expected, CT15 reacted with low levels of mouse APP in untransfected N2a cells (Figure 2, lane 1) and high, but variable levels of full-length ~100 and 105 kDa polypeptides representing synthetic and mature forms of human APP-695, respectively, in each of the cell lines (Figure 2). [^{35}S]-methionine pulse-labelling, immunoprecipitation, and phosphorimaging analysis revealed that relative biosynthetic rates of human APP in each of the lines were indistinguishable from the steady-state analysis shown in Figure 2 (data not shown).

Aβ in Conditioned Medium of Cell Lines

The levels of Aβ1–40 and Aβ1–42(43) species that accumulated in the conditioned medium of N2a cells coexpressing human APP and human PS1 were quantified using a well characterized BAN-50/BA-27 and BAN-50/BC-05 sandwich ELISA assay that specifically detects Aβ1–40 and Aβ1–42(43), respectively (Suzuki et al., 1994; Gravina et al., 1995; Scheuner et al., 1996). In view of the differing steady-state levels of human APP and human PS1 (or PS1 variants) and clonal variability in Aβ secretion, we chose to calculate the ratio of Aβ1–42(43) to Aβ1–40 (i.e., the Aβ42/40 ratio), instead of comparing the absolute levels of Aβ for each sample (Table 1). The

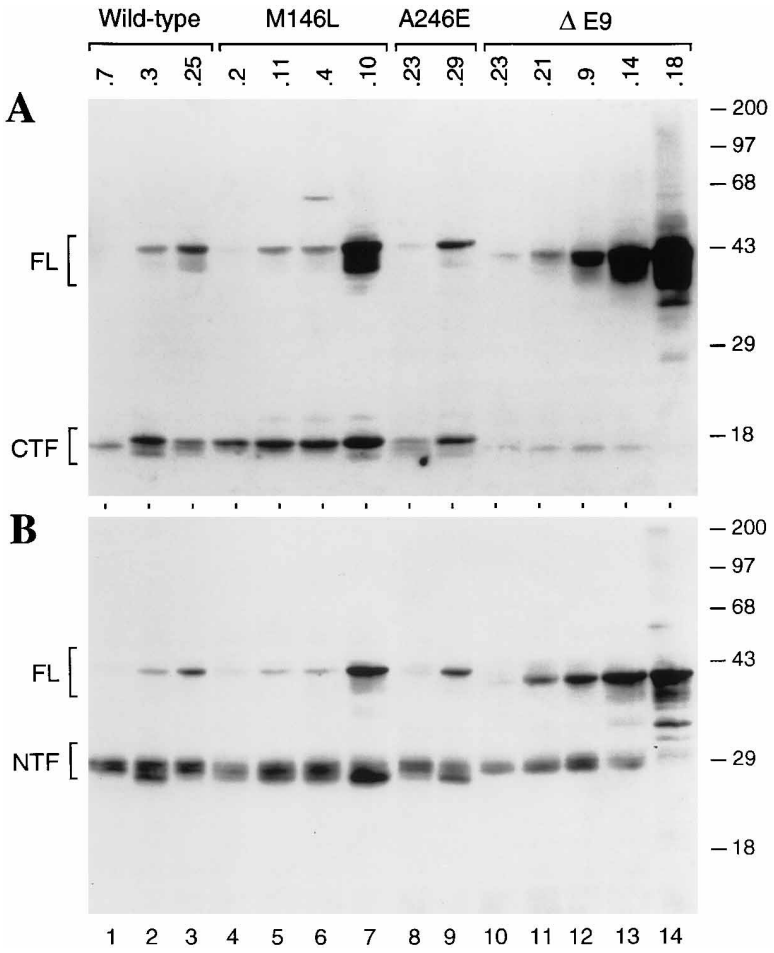

Figure 1. PS1 Expression in Stable N2a Cells

Mouse N2a neuroblastoma cells were cotransfected with expression plasmids encoding wild-type human APP-695 and wild-type human PS1, PS1M146L, PS1A246E, or PS1ΔE9. Detergent lysates (25 μg) were fractionated by SDS–polyacrylamide gel electrophoresis (PAGE) and expression of PS1 was analyzed by immunoblotting with PS1Loop antiserum (A) and N-terminal Ab14 antiserum (B). Note that αPS1Loop antiserum detects mouse PS1 at about 40% efficiency of human PS1 (Thinakaran et al., 1996). The positions of full-length PS1 (FL), C-terminal and N-terminal PS1-derived fragments (CTF and NTF, respectively) are marked.

statistical significance was calculated using the nonparametric Mann-Whitney test. The Aβ42/40 ratio in medium of N2a lines expressing human APP alone, or in combination with wild-type human PS1, were comparable (0.093 ± 0.004 and 0.100 ± 0.006, respectively). In this regard, despite an ~3-fold difference in the level of human PS1 expression between lines wt.3 and wt.25 (Figures 1A and 1B, lanes 2 and 3), the Aβ42/40 ratio in these lines were quite comparable (0.094 ± 0.006 and 0.106 ± 0.011, respectively). However, stable lines expressing the M146L (Figures 1A and 1B, lanes 4–7), A246E (Figures 1A and 1B, lanes 8 and 9), or ΔE9 (Figures 1A and 1B, lanes 10–14) PS1 variants exhibited significantly higher Aβ42/40 ratios relative to wild-type lines (0.154 ± .011 versus 0.098 ± .004, P = 0.0102). Significantly, the Aβ42/40 ratios were higher in seven lines that expressed mutant PS1 (i.e., ML.2, ML.11, ML.4, AE.23, AE.29, ΔE9.23, and ΔE9.21) at levels lower than, or equivalent to, wild-type human PS1 in lines wt.3 and wt.25 (0.128 ± 0.004 versus 0.1 ± 0.006, respectively; P = .0405). Interestingly, and for reasons not presently clear, an ~2-fold increase in expression of PS1ΔE9 in line ΔE9.9 compared with line ΔE9.21 (Figure 1A, lanes 10 and 11) resulted in a remarkable increase in the Aβ42/40 ratio (0.199 ± 0.004 versus 0.113 ± 0.003). However, further increases in the expression of the ΔE9 PS1 variant (Figure 1A, lanes 13 and 14) did not significantly elevate the Aβ42/40 ratio. Notably, the Aβ42/40 ratio for

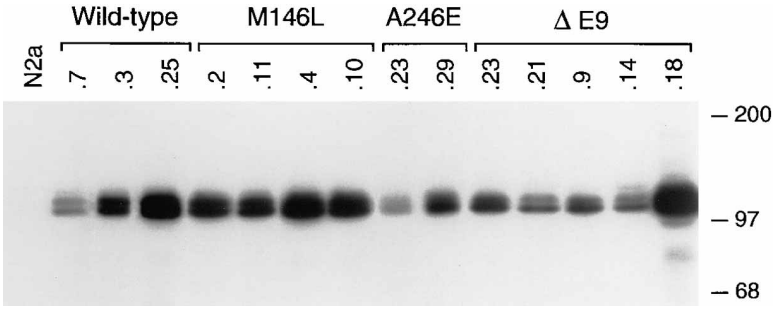

Figure 2. APP Expression in Stable N2a Cells

Detergent lysates (25 μg) prepared from untransfected N2a cells (N2a) and stable N2a lines coexpressing human wild-type APP and human PS1 polypeptides (wild-type PS1, PS1M146L, A246E, or PS1ΔE9) were fractionated by SDS–PAGE, and APP expression was examined by immunoblotting with CT15 antiserum.

Table 1. Ratio of Aβ1–42(43)/Aβ1–40 Species Secreted by Stable N2a Lines

N2a Line	Ratio of Aβ1–42(43)/Aβ1–40 Mean ± SEM	Number of Experiments
Wild-Type PS1 Lines		
(0.098 ± 0.004)		
wt.7	0.093 ± 0.004	4
wt.3	0.094 ± 0.003	6
wt.25	0.1060 ± 0.011	6
PS1M146L Lines		
(0.143 ± 0.019; $P = 0.0339$[a])		
ML.2	0.130 ± 0.007	6
ML.11	0.131 ± 0.009	6
ML.4	0.113 ± 0.007	6
ML.10	0.200 ± 0.011	6
PS1A246E Lines		
(0.135 (mean))		
AE.23	0.133 ± 0.012	6
AE.29	0.138 ± 0.016	6
PS1ΔE9 Lines		
(0.170 ± 0.019; $P = 0.0253$[a])		
ΔE9.23	0.137 ± 0.005	6
ΔE9.21	0.113 ± 0.004	6
ΔE9.9	0.199 ± 0.004	4
ΔE9.14	0.195 ± 0.010	6
ΔE9.18	0.206 ± 0.011	6

All mutant lines average 0.154 ± 0.011; $P = 0.0102$.
[a] P values were calculated by nonparametric Mann-Whitney test.

a line expressing the highest levels of the M146L variant (ML.10; Figure 1, lane 7) was 0.200 ± 0.001. In this instance, high levels of full-length M146L PS1 also accumulated.

At present, the relative contributions of full-length mutant PS1 or its fragments to Aβ42/40 production is unsettled. We reported that the preponderant PS1 species in vivo are its endoproteolytic derivatives (Thinakaran et al., 1996); in stably transfected cells, it is conceivable that accumulated full-length mutant PS1 may elevate the Aβ42/40 ratios in a manner that is nonphysiologic. However, it is quite clear that in lines expressing different mutant PS1 with nearly undetectable levels of accumulated full-length mutant PS1 (lines ML.2, AE.23, and ΔE9.23), the Aβ42/40 ratio averaged 0.133 compared with wild-type PS1-expressing lines that exhibited an Aβ42/40 ratio of 0.1, despite the accumulation of full-length wild-type PS1.

Expression of Human PS1 and Human APP in Transgenic Mice

To examine the influence of mutant PS1 on Aβ42/40 ratios in an in vivo setting, we examined Aβ42/40 ratios in the brains of transgenic mice expressing wild-type or mutant PS1. Mice expressing either wild-type Hu PS1 or the FAD-linked A246E PS1 variant were mated to transgenic mice expressing a chimeric Mo/Hu APP-695swe (APPswe) polypeptide. The APPswe cDNA was created by replacing sequences encoding the Aβ domain of murine APP with the cognate sequences from Hu APP, thus allowing examination of the influence of PS1 on human Aβ. All transgenes were transcriptionally dependent upon the murine prion promoter (MoPrP) vector (Thinakaran et al., 1996). The levels of human Aβ peptides in brain homogenates of transgenic animals were determined using a quantitative sandwich ELISA assay, described above (Suzuki et al., 1994; Gravina et al., 1995; Scheuner et al., 1996).

Our previous investigations of PS1 expression in transgenic mice revealed that 43 kDa human PS1 is proteolytically processed to generate ~27 kDa N-terminal and ~17 kDa C-terminal derivatives, which accumulate to equivalent levels (Thinakaran et al., 1996). We examined the expression of the A246E PS1 variant in total SDS extracts of brains of transgenic mice with Ab14, a polyclonal serum specific for amino acids 3–15 of human and mouse PS1 and mAb N-term, a monoclonal antibody (mAb) specific for PS1 N-terminal epitopes (see below; Figure 3B). We show that 43 kDa PS1-A246E is cleaved to generate 27 kDa derivatives (Figures 3A and 3B, lanes 5 and 6), which comigrated with N-terminal derivatives from human PS1 (Figure 3A, lanes 7 and 8). Notably, the A246E mutation is predicted to reside in the 27 kDa N-terminal fragment. Parallel immunoblot studies with antiserum to sequences in the loop domain of PS1 (Thinakaran et al., 1996) demonstrated the presence of C-terminal 17 kDa derivatives generated from the mutant PS1 polypeptide (data not shown). Thus, the A246E mutation does not conspicuously alter proteolytic processing of the PS1 variant in brain, consistent with our findings in stably transfected N2a cells (see above).

In the brains of mice from wild-type PS1 mice (line S8-4), we observed high levels of accumulated full-length 43 kDa species. In earlier studies, we demonstrated that human PS1 mRNA is highly overexpressed in the brains of line S8-4, and we argued that accumulation of full-length human PS1 is the result of high synthetic rates of transgene-encoded mRNAs (Thinakaran et al., 1996). In those studies, we also documented that the levels of accumulated N-terminal human PS1 fragments in brains of line S8-4 were indistinguishable from the levels of accumulated N-terminal fragments in brains of independent lines of mice expressing human PS1 mRNA at levels ~10- to 20-fold lower than mRNA in line S8-4 (Thinakaran et al., 1996). From these analyses, we concluded that accumulation of the PS1 endoproteolytic derivatives is highly regulated and saturable. In contrast to line S8-4, very little full-length A246E PS1 accumulated in the brains of line N5, consistent with Northern blot analyses, which demonstrated that brain mRNA levels in line N-5 are ~3- to 5-fold lower than in line S8-4 (data not shown). Interestingly, the levels of accumulated N-terminal human PS1 fragments in brains of lines N5 and S8-4 are quite comparable, despite the accumulation of full-length wild-type PS1 in line S8-4.

Total APP levels in detergent extracts from the brains of the APPswe transgenic mice and mice coexpressing APPswe and Hu PS1 were examined by immunoblotting with CT15, an APP C-terminal specific antiserum; the CT-15 epitope is conserved in human and murine APP.

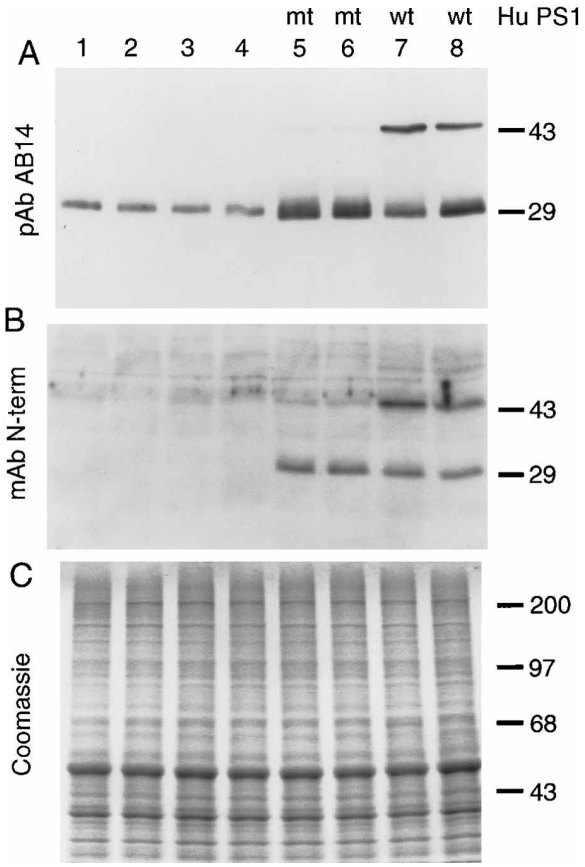

Figure 3. Expression of Wild-Type and Mutant Hu PS1 in Transgenic Mice

The cortex, hippocampus, and thalamus of brains from 2- to 3-month-old transgenic and nontransgenic littermates were homogenized as described in Experimental Procedures.

(A) and (B) We analyzed 50 μg of brain protein by immunoblot with N-terminal antibodies Ab14 and mAb N-term. Bound primary antibodies were revealed by [^{125}I]-protein A (primary mAb required prior to incubation with rabbit antiserum to mouse IgG). The mAb N-term specifically recognizes human PS1.

(C) A Coomassie-stained gel, run in parallel, demonstrates equal loading of brain protein extracts. Lanes 1 and 2, nontransgenic mice; lanes 3 and 4, transgenic mice harboring APPswe transgenes alone; lanes 5 and 6, transgenic mice harboring APPswe and mutant human PS1 transgenes; lanes 7 and 8, transgenic mice harboring APPswe and wild-type human PS1 transgenes.

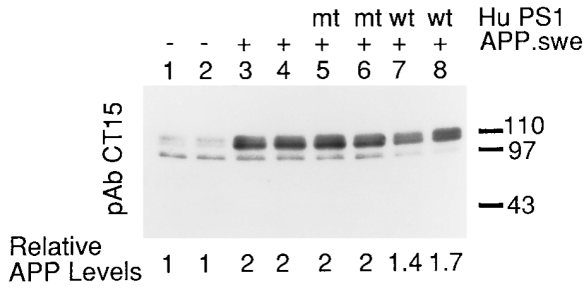

Figure 4. Expression of Mo/Hu APP-695swe in Transgenic Mice Coexpressing Wild-Type and Mutant Human PS1

Total SDS extracts of brain protein were analyzed by immunoblotting with CT15, an antibody that recognizes both murine and human APP. Mice harboring the APPswe transgene show an ~2 fold increase in APP immunoreactivity. Lanes 1 and 2, nontransgenic mice; lanes 3 and 4, transgenic mice harboring APPswe transgenes alone; lanes 5 and 6, transgenic mice harboring APPswe and mutant human PS1 transgenes; lanes 7 and 8, transgenic mice harboring APPswe and wild-type human PS1 transgenes.

We observed an increase in the levels of accumulated 100–110 kDa APP (Figure 4, lanes 3–8) compared with littermates lacking transgenes (Figure 4, lanes 1 and 2). Phosphorimaging analysis of CT-15 immunoblots indicated an ~2-fold increase in APP levels in mice harboring the APPswe transgene. Parallel analyses with mAb 6E10, specific for human Aβ sequences (Kim et al., 1988, 1990; Hsiao et al., 1995), confirmed the presence of humanized Aβ domains in the APPswe polypeptides (data not shown).

Aβ Levels in Brains of Transgenic Mice Coexpressing Human PS1 and Human APP

Levels of Aβ were measured in homogenates of brains from 2- to 3-month-old transgenic mice by quantitative sandwich ELISA assays, described above (Suzuki et al., 1994; Gravina et al., 1995; Scheuner et al., 1996). Although the absolute levels of Aβ1–40 and Aβ1–42(43) in the brains of transgenic mice varied considerably, coexpression of mutant PS1 with APPswe disproportionately elevated the concentration of Aβ1–42(43) relative to Aβ1–40 (Figure 5); the Aβ42/40 ratio shifted from a mean of 0.215 (SE = 0.011) in littermate mice expressing APPswe alone (Group A) to a mean of .305 (SE = 0.014) in mice expressing both APPswe and mutant PS1. Importantly, the Aβ42/40 ratios in mice coexpressing mutant PS1 and APPswe did not overlap with those for mice expressing APPswe alone; nonparametric Mann-Whitney statistical analyses revealed that the difference between the two groups was highly significant ($P = 0.006$). Because we observed significant variability in absolute levels of total Aβ42/40 in the cohort of APPswe littermates (Group A), we repeated the analyses on a cohort of APPswe animals alone (APPswe B6 n1 generation; see Experimental Procedures), which were aged 7 months (Group B). The ratios of Aβ42/40 in the brains from the two groups of APPswe mice (Groups A and B) were very similar (0.215 and 0.212, respectively). Nonparametric Mann-Whitney analyses revealed that the 50% increase in the Aβ42/40 ratio in the brains of mice expressing both APPswe and mutant Hu PS1 as compared with mice expressing APPswe alone (Groups A and B) was highly significant ($P = 0.001$). Thus, despite the variability in total Aβ levels, the effects of mutant Hu PS1 were sufficiently robust to cause detectable, and highly statistically significant, increases in the Aβ42/40 ratio.

To examine the effects of human wild-type PS1 on Aβ42/40 ratios, we examined the brains of two mice coexpressing APPswe and wild-type human PS1. We observed that the Aβ42/40 ratio in these animals was 0.192, a value not statistically different from the mice expressing APPswe alone (Figure 5). Thus, increasing PS1 expression alone is not sufficient to alter the Aβ42/40 ratio. Moreover, a significant shift in the Aβ42/40 ratio ($P = 0.05$) was observed when we compared values for

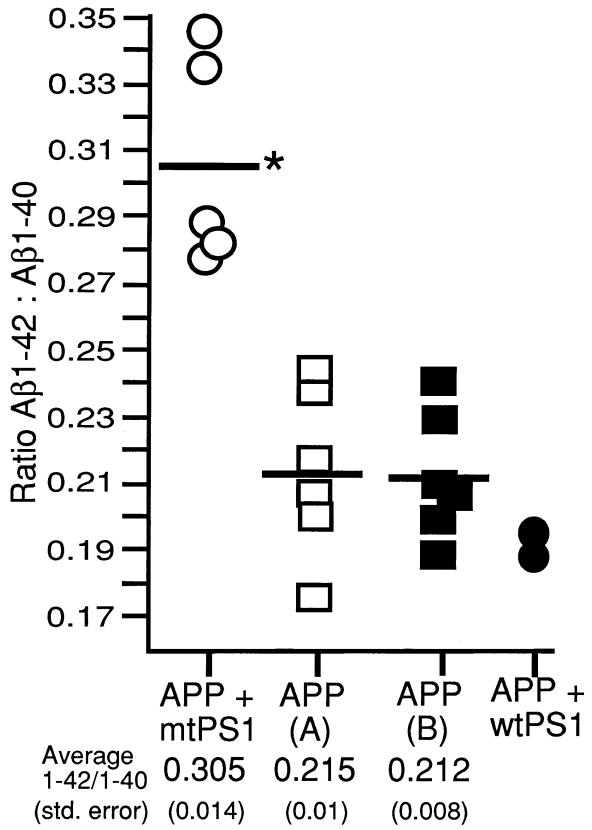

Figure 5. Scatter Plot of Aβ1–42(43) to Aβ1–40 Ratios

Data on Aβ1–42(43) to Aβ1–40 ratios are displayed to illustrate the lack of overlap between values in the APPswe + mutant human PS1 transgenics versus APPswe alone and APPswe + wild-type human PS1 mice. Horizontal bars mark the average value for Aβ1–42(43) to Aβ1–40 ratios. Asterisk: this average value is significantly higher than the average value for APPswe mice ($P = 0.001$) and APPswe × wild-type human PS1 mice ($P = 0.05$).

mice coexpressing wild-type PS1 and APPswe (0.192) and mice coexpressing mutant PS1 and APPswe (0.305). The higher level of transgene expression in wild-type PS1 mice (line S8-4) underscores the significance of these observations and leads us to conclude that only mutant Hu PS1 influences APP processing in a manner that enhances Aβ1–42(43) production.

Discussion

Mutations in *PS1* and *PS2* cosegregate with the majority of pedigrees with early-onset FAD, but the molecular mechanism(s) by which FAD-linked PS1 and PS2 variants cause AD are unclear. The absence of nonsense or frameshift mutations leading to truncated PS1/PS2 support the notion that AD is caused not by the loss, but by the gain, of deleterious properties of the mutant polypeptides. In this regard, recent studies indicate that conditioned medium from fibroblasts or plasma of affected members of pedigrees with *PS1*/*PS2*-linked mutations show a significant increase in the ratio of Aβ1–42(43)/Aβ1–40 relative to unaffected family members (Scheuner et al., 1996). These data suggest that the FAD-linked mutations cause AD by increasing the extracellular concentration of highly amyloidogenic Aβ1–42(43) species, thus fostering Aβ amyloid deposition in the brain.

To examine directly the influences of wild-type and mutant PS1 on Aβ1–40 and Aβ1–42(43) production, we generated stable mouse neuroblastoma (N2a) cell lines that constitutively express human APP in combination with human PS1 or FAD-linked PS1 variants. We extended these investigations to analyze the Aβ1–42(43) to Aβ1–40 ratio in the CNS of transgenic mice that express a chimeric APP (APPswe) in combination with wild-type PS1 or the FAD-linked A246E PS1 variant.

Our findings provide the first demonstration of a *bona fide* effect of wild-type and mutant PS1 on Aβ42(43) production in vitro and in vivo and offer important insights into the pathogenetic mechanism of PS1-linked FAD. First, we document that the ratio of Aβ1–42(43)/Aβ1–40 in the medium of independent cell lines expressing variable levels of either the A246E, the M146L, or ΔE9 PS1 variants is uniformly elevated compared with medium of cells expressing wild-type PS1. In these studies, elevated extracellular Aβ42(43) accumulation, mediated by mutant PS1, occurred in independent lines that express the M146L, A246E, or ΔE9 variants at levels lower than, or comparable with, lines expressing human wild-type PS1. Second, we document that the ratio of Aβ1–42(43) to Aβ1–40 in the brains of young transgenic animals coexpressing APPswe and mutant PS1 is elevated by 50% compared with transgenic mice expressing APPswe alone or transgenic mice coexpressing wild-type Hu PS1 and APPswe. At this time, amyloid deposition and associated neuropathological abnormalites have not been detected in the brains of older mice expressing either APPswe alone (14 months), mutant PS1 alone (8 months), or young animals coexpressing APPswe and mutant PS1 (D. R. B. and M. K. L., unpublished data). Hence, the alterations in Aβ1–42(43)/Aβ1–40 ratios detected in the brains of our young animals coexpressing APPswe and mutant PS1 are not the consequence of pathogenic processes, but rather are indicative of fundamental changes in the processing of APP. Collectively, the data obtained from stably transfected cells and brains of transgenic mice provide compelling support for the view that one mechanism by which mutant PS1 causes AD is the acquisition (or enhancement) of property(ies) that influence APP processing in a manner that leads to increased extracellular concentrations of Aβ1–42(43).

Our findings are notable in view of several lines of evidence in support of the idea that Aβ1–42(43) plays a critical role in the pathogenesis of AD: first, biophysical studies demonstrate that Aβ1–42 has rapid nucleation and aggregation kinetics (Jarrett and Lansbury, 1993); second, mass spectrometric analyses of purified amyloid plaques revealed that Aβ1–42 is the principal component of amyloid deposits (Roher et al., 1993); third, cells expressing FAD-linked APP with missense mutations at position 717 (of APP-770) secrete high levels of Aβ1–42(43) (Suzuki et al., 1994); and fourth, biochemical and immunocytochemical studies of brains from patients with AD (Iwatsubo et al., 1994; Gravina et al., 1995) and Down's Syndrome (Iwatsubo et al., 1995; Lemere

et al., 1996a) using end-specific antibodies revealed that Aβ species terminating at residue 42(43) occur early and selectively in both diffuse and compact amyloid plaques. Significantly, recent studies (Lemere et al., 1996b) have demonstrated abundant Aβ42(43) deposition in the cerebral cortex and cerebellum of individuals with a PS1-linked E280A mutation with amyloid burdens that far exceeds that described for individuals homozygous for apoE4 alleles (Roses, 1994; Hyman et al., 1995). All of these lines of evidence indicate that Aβ1–42(43) is a critical peptide in the pathogenesis of amyloid deposition. These converging lines of evidence, in conjunction with our demonstration that mutant PS1 influences APP processing in vitro and in vivo, are consistent with the hypothesis that elevated extracellular concentrations of amyloidogenic Aβ1–42(43) peptides precipitate disease in PS1-linked FAD.

Experimental Procedures

Generation of PS1 Expression Vectors

A cDNA-encoding human PS1 was generated as described (Slunt et al., 1995). PS1 cDNA encoding the A246E substitution was generated by RT–PCR of cytoplasmic RNA isolated from skin fibroblasts of a patient harboring the A246E mutation (NIA Cell Repository #AG06848B) using the primer pair, hAD3-ATG-Kpn (GGGGTACCATGACAGAGTT ACCTGCAC) and hAD3-R-3′UTR (CCGGGATCCATGGGATTCTAAC CGC). PCR product was digested with Asp-718 and BamHI, and ~1.4 kB PS1 cDNA was gel purified and ligated to Bluescript KS+ vector (Stratagene, La Jolla, CA) previously digested with Asp-718 and BamHI, to generate phPS1A246E. The cDNA were sequenced in their entirety using a Sequenase (U. S. B, Cleveland, OH). To generate human PS1 cDNA encoding the M146L substitution, we used a four-way PCR strategy with two primer pairs and full-length PS1 cDNA as template. The primer pairs for the initial PCR reactions were hAD3-M146LF (GTC ATTGTTGTCCTGACTATCCTCCTG)/hAD3-R284 (GAGGAGTAAATGA GAGCTGG) and hAD3-M146LR (CAGGAGGATAGTCAGGACAACAAT GAC)/hAD3-237F (CAGGTGGTGGAGCAAGATG). PCR products from each reaction were gel purified, combined, and subject to a second round of PCR with primers hAD3-237F and hAD3-R284. The resulting product was digested with KasI and PflMI and an ~300 bp gel-purified fragment was ligated to KasI/PflM1-digested phPS1 to generate phPS1M146L. The inserts and junctions were sequenced using Sequenase (U. S. B, Cleveland, OH). The strategy for generating cDNA encoding PS1 lacking exon 9 (amino acids 290–319) was described previously (Thinakaran et al., 1996). Sequences encoding PS1 variants were subcloned downstream of mouse prion promoter in plasmid MoPrP. Xho (Thinakaran et al., 1996), to generate MoPrP. PS1 expression plasmids.

Antibodies

Two antibodies directed against N-terminal epitopes of PS1 were used in this study: Ab14 is a polyclonal serum specific for amino acids 3–15 of human and mouse PS1 (Thinakaran et al., 1996), and mAb N-term is a concentrated cell culture supernatant from a rat myeloma primed with a chimeric protein consisting of the N-terminal 80 amino acids of human PS1 fused to bacterial glutathione S-transferase. αPS1Loop, an antiserum that specifically reacts with epitopes in the hydrophilic loop domain of PS1 (amino acids 263–407) (Thinakaran et al., 1996) was used to detect PS1 C-terminal derivatives.

For Western blot analysis, detergent lysates were prepared from cells and transgenic mouse brains as described previously (Thinakaran et al., 1996). The steady-state expression of PS1 and APP in cultured cells and mouse brain was examined by Western blot analysis using PS1-specific, αPS1Loop, and Ab14 antisera, and APP-specific CT15 antisera (Sisodia et al., 1993). Human PS1 in transgenic mouse brain was detected with mAb N-term. The blots were incubated with [^{125}I]protein A (Dupont/NEN, Wilmington, DE) and bound radioactivity was quantified by phosphorimaging (Molecular Dynamics, Sunnyvale, CA).

Generation of Stable Cell Lines Expressing PS1 and APP

Stable mouse N2a neuroblastoma cells were generated by cotransfecting 5 μg MoPrP. PS1 expression plasmids encoding human wild-type PS1, PS1M146L, PS1A246E, or PS1ΔE9, with 0.5 μg of cDNA encoding human wild-type APP-695 in a CMV expression vector, pCB6 (Lo et al., 1994). Expression of human PS1 in G418-resistant lines was determined by Western blot analysis with polyclonal αPS1Loop and Ab14 antisera (Thinakaran et al., 1996). Expression of human APP was determined by Western blot analysis with CT15 antiserum. One N2a line expressing APP and undetectable levels of human PS1 (wt.7), two wild-type PS1 lines (wt.3 and wt.25), four PS1M146L lines (ML.2, ML.4, ML.10, and ML.11), two PS1A246E lines (AE.23 and AE.29), and five PS1ΔE9 lines (ΔE9.9, ΔE9.14, ΔE9.18, ΔE9.21, and ΔE9.29) were used in this study.

Generation of Transgenic Mice

Transgenic mice expressing wild-type Hu PS1 were previously described (Thinakaran et al., 1996). In the present study, we used a line of transgenic mice expressing very high levels of wild-type Hu PS1 (line S8-4) (Thinakaran et al., 1996). To generate transgenic mice expressing the A246E PS1 variant, we injected pronuclei with linealized expression plasmid, MoPrP. A246E, described above. All Hu PS1 transgenic mice were maintained as C3H/HeJ × C57BL/6J hybrids.

To generate cDNA encoding Mo/Hu APP-695swe, a PCR-based strategy was utilized in which the oligonucleotide primers encoded the "Swedish" missense mutations and contained appropriate restriction endonuclease sites to allow for the construction of chimeric APP. The cDNA were sequenced prior to insertion into the MoPrP. Xho vector. Mice harboring the APPswe transgene were initially generated in F2 hybrids of C3H/HeJ × C57BL/6J mice. The F3 progeny of these matings were subsequently mated to C57BL/6J for one generation (APPswe B6n1) before mating to mice harboring PS1 transgenes (all of which were F3 progeny of C3H/HeJ × C57BL/6J matings).

Analysis of Aβ1–40 and Aβ1–42(43) Secreted by Stable N2a PS1/APP Lines

Stable N2a lines were plated 1×10^6 cells/60 mm dish and maintained in 1:1 OptiMEM (GIBCO-BRL, Bethesda, MD) and Dulbecco's modified Eagle's medium supplemented with 10% fetal bovine serum. The following day, culture medium was replaced with fresh medium containing 10 mM butyrate (to induce transcription of the CMV promoter-driven human APP cDNA) (Lo et al., 1994). The conditioned medium was collected 24 hr later and stored frozen at −70°C. The samples were coded in order to facilitate a blinded comparison. Aliquots of conditioned medium were analyzed by BAN-50/BA-27 or BAN-50/BC-05 sandwich ELISA assays essentially as previously described (Suzuki et al., 1994; Scheuner et al., 1996) to measure Aβ1–40 and Aβ1–42(43), respectively.

Analysis of Aβ1–40 and Aβ1–42(43) in Brain Tissue

Approximately 150 mg of tissue was dounce homogenized (6 strokes) in 1 ml of 70% formic acid. Homogenates were centrifuged at 100,000 × g for 1 hr to remove particulate material. The supernatant was recovered and neutralized with a 20-fold dilution in 1 M Tris base. Following neutralization, 100 μl of the sample was mixed with 50 μl of EC buffer (0.02 M sodium phosphate, 0.2 mM EDTA, 0.4 M NaCl, 0.2% BSA, 0.05% CHAPS, 0.4% Block-Ace, 0.05% sodium azide [pH 7.0]) and analyzed directly using the BAN-50/BA27 and BAN-50/BC05 sandwich ELISA system (Suzuki et al., 1994; Gravina et al., 1995; Hsiao et al., 1995; Scheuner et al., 1996). The values obtained were calculated by comparison with the absorbances obtained from a standard curve of synthetic Aβ1–40 and Aβ1–42 (Bachem, King of Prussia, PA), adjusted for sample dilution, and converted to pmols/g wet weight tissue.

Acknowledgments

We thank Mr. Marek Fischer and Dr. Charles Weissmann for the pPrPHG plasmid, which contained a modified murine prion protein

gene from which the MoPrP. Xho vector was generated. We also thank Ms. Debbie Swing for her technical assistance in the production of transgenic mice and Mr. Yuri McKee, Ms. Liesl Awalt, Ms. Luba Romansteva, and Mr. Dustin Englekin for help in screening transgenic mice. We thank Drs. Mary Savage and Barry Greenberg (Cephalon, Inc.) for their collaborative efforts during the early stages of the cell culture studies. This work was supported by the U. S. Public Health Service, National Institute of Health grants NIH AG05146, NS 20471 (S. S. and D. L. P.); AG05689 (M. S.); AG11508 and AG09464 (S. E. G.); P01AG14633-01, AG12685-04, and AG06656 (S. G. Y); and by grants from the Adler Foundation (G. T. and S. S. S.), the Develbiss Fund (D. R. B., D. L. P., and S. S. S.), and the Alzheimer's Association (D. R. B. and S. S. S.) and the National Cancer Center Institute, DHHS, under contract with Advanced Bioscience Laboratories. D. L. P. is the recipient of a Javitz Neuroscience Investigator Award (NIH NS10580); D. L. P and D. R. B are the recipients of a Leadership and Excellence in Alzheimer's Disease (LEAD) Award (NIH AG07914); S. S. S. is the recipient of an Alzheimer's Association Zenith Award.

The costs of publication of this article were defrayed in part by the payment of page charges. This article must therefore be hereby marked *"advertisement"* in accordance with 18 USC Section 1734 solely to indicate this fact.

Received August 29, 1996; revised October 21, 1996.

References

Alzheimer's Disease Collaborative Group. (1995). The structure of the presenilin 1 (*S182*) gene and identification of six novel mutations in early onset AD families. Nature Genet. *11,* 219–222.

Boteva, K., Vitek, M., Mitsuda, H., de Silva, H., Xu, P.-T., Small, G., and Gilbert, J.R. (1996). Mutation analysis of presenilin 1 gene in Alzheimer's disease. Lancet *347*, 130–131.

Burdick, D., Soreghan, B., Kwon, M., Kosmoski, J., Knauer, M., Henschen, A., Yates, J., Cotman, C., and Glabe, C. (1992). Assembly and aggregation properties of synthetic Alzheimer's A4/β amyloid peptide analogs. J. Biol. Chem. *267,* 546–554.

Cai, X.-D., Golde, T.E., and Younkin, S.G. (1993). Release of excess amyloid β protein from a mutant amyloid β protein precursor. Science *259,* 514–516.

Campion, D., Flaman, J.M., Brice, A., Hannequin, D., Dubois, B., Martin, C., Moreau, V., Charbonnier, F., Didierjean, O., Tardieu, S., Penet, C., Puel, M., Pasquier, F., Ledoze, F., Bellis, G., Calenda, A., Heilig, R., Martinez, M., Mallet, J., Bellis, M., Clergetdarpoux, F., Agid, Y., and Frebourg, T. (1995). Mutations of the presenilin 1 gene in families with early-onset Alzheimer's disease. Hum. Mol. Genet. *4*, 2373–2377.

Chapman, J., Asherov, A., Wang, N., Treves, T.A., Korczyn, A.D., and Goldfarb, L.G. (1995). Familial Alzheimer's disease associated with S182 codon 286 mutation. Lancet *346*, 1040.

Chartier-Harlin, M.-C., Crawford, F., Houlden, H., Warren, A., Hughes, D., Fidani, L., Goate, A., Rossor, M., Roques, P., Hardy, J., and Mullan, M. (1991). Early-onset Alzheimer's disease caused by mutations at codon 717 of the β-amyloid precursor protein gene. Nature *353*, 844–846.

Citron, M., Oltersdorf, T., Haass, C., McConlogue, L., Hung, A.Y., Seubert, P., Vigo-Pelfrey, C., Lieberburg, I., and Selkoe, D.J. (1992). Mutation of the β-amyloid precursor protein in familial Alzheimer's disease increases β-protein production. Nature *360,* 672–674.

Cruts, M., Backhovens, H., Wang, S.Y., Vangassen, G., Theuns, J., Dejonghe, C., Wehnert, A., Devoecht, J., deWinter, G., Cras, P., Bruyland, M., Datson, N., Weissenbach, J., Dendunnen, J.T., Martin, J.J., Hendriks, L., and Vanbroeckhoven, C. (1995). Molecular genetic analysis of familial early-onset Alzheimer's disease linked to chromosome 14Q24.3. Hum. Mol. Genet. *4*, 2363–2371.

Goate, A., Chartier-Harlin, M.-C., Mullan, M., Brown, J., Crawford, F., Fidani, L., Giuffra, L., Haynes, A., Irving, N., James, L., Mant, R., Newton, P., Rooke, K., Roques, P., Talbot, C., Pericak-Vance, M., Roses, A., Williamson, R., Rossor, M., Owen, M., and Hardy, J. (1991). Segregation of a missense mutation in the amyloid precursor protein gene with familial Alzheimer's disease. Nature *349*, 704–706.

Gravina, S.A., Ho, L., Eckman, C.B., Long, K.E., Otvos, L., Jr., Younkin, L.H., Suzuki, N., and Younkin, S.G. (1995). Amyloid β protein (Aβ) in Alzheimer's disease brain. J. Biol. Chem. *270*, 7013–7016.

Hendriks, L., van Duijn, C.M., Cras, P., Cruts, M., Van Hul, W., van Harskamp, F., Warren, A., McInnis, M.G., Antonarakis, S.E., Martin, J.-J., Hofman, A., and Van Broeckhoven, C. (1992). Presenile dementia and cerebral haemorrhage linked to a mutation at codon 692 of the β-amyloid precursor protein gene. Nature Genet. *1,* 218–221.

Hsiao, K.K., Borchelt, D.R., Olson, K., Johannsdottir, R., Kitt, C., Yunis, W., Xu, S., Eckman, C., Younkin, S., Price, D., Iadecola, C., Clark, H.B., and Carlson, G. (1995). Age-related CNS disorder and early death in transgenic FVB/N mice overexpressing Alzheimer amyloid precursor proteins. Neuron *15,* 1203–1218.

Hyman, B.T., West, H.L., Rebeck, G.W., Buldyrev, S.V., Mantegna, R.N., Ukleja, M., Havlin, S., and Stanley, H.E. (1995). Quantitative analysis of senile plaques in Alzheimer disease: observation of log-normal size distribution and molecular epidemiology of differences associdated with apolipoprotein E genotype and trisomy (Down syndrome). Proc. Natl. Acad. Sci. USA *92*, 3586–3590.

Iwatsubo, T., Odaka, A., Suzuki, N., Mizusawa, H., Nukina, N., and Ihara, Y. (1994). Visualization of Aβ42(43)-positive and Aβ40-positive senile plaques with end-specific Aβ-monoclonal antibodies: evidence that an initially deposited Aβ species is Aβ1–42(43). Neuron *13*, 45–53.

Iwatsubo, T., Mann, D.M.A., Odaka, A., Suzuki, N., and Ihara, Y. (1995). Amyloid β protein (Aβ) deposition: Aβ42(43) precedes Aβ40 in Down syndrome. Ann. Neurol. *37*, 294–299.

Jarrett, J.T., and Lansbury, P.T., Jr. (1993). Seeding one-dimensional crystallization of amyloid: a pathogenic mechanism in Alzheimer's disease and scrapie? Cell *73*, 1055–1058.

Jarrett, J.T., Berger, E.P., and Lansbury, P.T., Jr. (1993). The carboxy terminus of the β amyloid protein is critical for the seeding of amyloid formation: implications for the pathogenesis of Alzheimer's disease. Biochem *32,* 4693–4697.

Kim, K.S., Miller, D.L., Sapienze, V.J., Chang, C.J., Grundke-Iqbal, I., Currie, J.R., and Wisniewski, H.M. (1988). Production and characterization of monoclonal antibodies reactive to synthetic cerebrovascular amyloid peptide. Neurosci. Res. Commun. *2,* 121–130.

Kim, K.S., Wen, G.Y., Bancher, C., Chen, C.M.J., Sapienza, V.J., Hong, H., and Wisniewski, H.M. (1990). Detection and quantitation of amyloid B-peptide with 2 monoclonal antibodies. Neurosci. Res. Commun. *7,* 113–122.

Lemere, C.A., Blusztajn, J.K., Yamaguchi, H., Wisniewski, T., Saido, T.C., and Selkoe, D.J. (1996a). Sequence of deposition of heterogeneous amyloid β-peptides and APO E in Down syndrome: implications for initial events in amyloid plaque formation. Neurobiol. Dis. *3*, 16–32.

Lemere, C.A., Lopera, F., Koski, K.S., Lendon, C.L., Ossa, J., Saido, T.C., Yamaguchi, H., Ruiz, A., Martinez, A., Madrigal, L., Hincabie, L., Arango, J.C., Anthony, D.C., Koo, E.H., Goate, A.M., Selkoe, D.J., and Arango, J.C., V. (1996b). The E280A presenilin 1 Alzheimer mutation produces increased Aβ42 deposition and severe cerebellar pathology. Nature Med. *2*, 1146–1150.

Levy-Lahad, E., Wasco, W., Poorkaj, P., Romano, D.M., Oshima J., Pettingell, W.H., Yu, C.-E., Jondro, P.D., Schmidt, S.D., Wang, K., Crowley, A.C., Fu, Y.-H., Guenette, S.Y., Galas, D., Nemens, E., Wijsman, E.M., Bird, T.D., Schellenberg, G.D., and Tanzi, R.E. (1995a). Candidate gene for the chromosome 1 familial Alzheimer's disease locus. Science *269*, 973–977.

Levy-Lahad, E., Wijsman, E.M., Nemens, E., Anderson, L., Goddard, K.A.B., Weber, J.L., Bird, T.D., and Schellenberg, G.D. (1995b). A familial Alzheimer's disease locus on chromosome 1. Science *269*, 970–973.

Lo, A.C.Y., Haass, C., Wagner, S.L., Teplow, D.B., and Sisodia, S.S. (1994). Metabolism of the "Swedish" amyloid precursor protein variant in Madin-Darby canine kidney cells. J. Biol. Chem. *269*, 30966–30973.

Mullan, M., Crawford, F., Axelman, K., Houlden, H., Lilius, L., Winblad, B., and Lannfelt, L. (1992). A pathogenic mutation for probable

Alzheimer's disease in the APP gene at the N-terminus of β-amyloid. Nature Genet. *1*, 345–347.

Naruse, S., Igarashi, S., Kobayashi, H., Aoki, K., Inuzuka, T., Kaneko, K., Shimizu, T., Iihara, K., Kojima, T., Miyatake, T., and Tsuji, S. (1991). Mis-sense mutation Val-Ile in exon 17 of amyloid precursor protein gene in Japanese familial Alzheimer's disease. Lancet *337*, 978–979.

Perez-Tur, J., Froelich, S., Prihar, G., Crook, R., Baker, M., Duff, K., Wragg, M., Busfield, F., Lendon, C., Clark, R.F., Roques, P., Fuldner, R.A., Johnston, J., Cowburn, R., Forsell, C., Axelman, K., Lilius, L., Houlden, H., Karran, E., Roberts, G.W., Rossor, M., Adams, M.D., Hardy, J., Goate, A., Lannfelt, L., and Hutton, M. (1995). A mutation in Alzheimer's disease destroying a splice acceptor site in the presenilin-1 gene. Neuroreport *7*, 297–301.

Rogaev, E.I., Sherrington, R., Rogaeva, E.A., Levesque, G., Ikeda, M., Liang, Y., Chi, H., Lin, C., Holman, K., Tsuda, T., Mar, L., Sorbi, S., Nacmias, B., Piacentini, S., Amaducci, L., Chumakov, I., Cohen, D., Lannfelt, L., Fraser, P.E., Rommens, J.M., and St George-Hyslop, P.H. (1995). Familial Alzheimer's disease in kindreds with missense mutations in a gene on chromosome 1 related to the Alzheimer's disease type 3 gene. Nature *376*, 775–778.

Roher, A.E., Lowenson, J.D., Clarke, S., Wolkow, C., Wang, R., Cotter, R.J., Reardon, I.M., Zurcher-Neely, H.A., Heinrikson, R.L., Ball, M.J., and Greenberg, B.D. (1993). Structural alterations in the peptide backbone of β-amyloid core protein may account for its deposition and stability in Alzheimer's disease. J. Biol. Chem. *268*, 3072–3083.

Roses, A.D. (1994). Apolipoprotein E affects the rate of Alzheimer's disease expression: β-amyloid burden is a secondary consequence dependent on APOE genotype and duration of disease. J. Neuropath. Exp. Neurol. *53*, 429–437.

Schellenberg, G.D. (1995). Genetic dissection of Alzheimer disease, a heterogeneous disorder. Proc. Natl. Acad. Sci. USA *92*, 8552–8559.

Scheuner, D., Eckman, C., Jensen, M., Song, X., Citron, M., Suzuki, N., Bird, T.D., Hardy, J., Hutton, M., Kukull, W., Larson, E., Levy-Lahad, E., Viitanen, M., Peskind, E., Poorkaj, P., Schellenberg, G., Tanzi, R., Wasco, W., Lannfelt, L., Selkoe, D., and Younkin, S. (1996). Secreted amyloid β-protein similar to that in the senile plaques of Alzheimer's disease is increased in vivo by the presenilin 1 and 2 and APP mutations linked to familial Alzheimer's disease. Nature Med. *2*, 864–870.

Sherrington, R., Rogaev, E.I., Liang, Y., Rogaeva, E.A., Levesque, G., Ikeda, M., Chi, H., Lin, C., Li, G., Holman, K., Tsuda, T., Mar, L., Foncin, J.-F., Bruni, A.C., Montesi, M.P., Sorbi, S., Rainero, I., Pinessi, L., Nee, L., Chumakov, I., Pollen, D., Brookes, A., Sanseau, P., Polinsky, R.J., Wasco, W., Da Silva, H.A.R., Haines, J.L., Pericak-Vance, M.A., Tanzi, R.E., Roses, A.D., Fraser, P.E., Rommens, J.M., and St George-Hyslop, P.H. (1995). Cloning of a gene bearing missense mutations in early-onset familial Alzheimer's disease. Nature *375*, 754–760.

Sisodia, S.S., Koo, E.H., Hoffman, P.N., Perry, G., and Price, D.L. (1993). Identification and transport of full-length amyloid precursor proteins in rat peripheral nervous system. J. Neurosci. *13,* 3136–3142.

Slunt, H.H., Thinakaran, G., Lee, M.K., and Sisodia, S.S. (1995). Nucleotide sequence of the chromosome 14-encoded S182 cDNA and revised secondary structure prediction. Amyloid: Int. J. Exp. Clin. Invest. *2*, 188–190.

St George-Hyslop, P.H, Haines, J., Rogaev, E., Mortilla, M., Vaula, G., Pericak-Vance, M., Foncin, J.-F., Montesi, M., Bruni, A., Sorbi, S., Rainero, I., Pinessi, L., Pollen, D., Polinsky, R., Nee, L., Kennedy, J., Macciardi, F., Rogaeva, E., Liang, Y., Alexandrova, N., Lukiw, W., Schlumpf, K., Tanzi, R., Tsuda, T., Farrer, L., Cantu, J.-M., Duara, R., Amaducci, L., Bergamini, L., Gusella, J., Roses, A., and Crapper McLachlan, D. (1992). Genetic evidence for a novel familial Alzheimer's disease locus on chromosome 14. Nature Genet. *2* 330–334.

Suzuki, N., Cheung, T.T., Cai, X.-D., Odaka, A., Otvos, L., Jr., Eckman, C., Golde, T.E., and Younkin, S.G. (1994). An increased percentage of long amyloid β protein secreted by familial amyloid β protein precursor (βAPP717) mutants. Science *264*, 1336–1340.

Thinakaran, G., Borchelt, D.R., Lee, M.K., Slunt, H.H., Spitzer, L., Kim, G., Ratovitski, T., Davenport, F., Nordstedt, C., Seeger, M., Hardy, J., Levey, A.I., Gandy, S.E., Jenkins, N.A, Copeland, N.G., Price, D.L., and Sisodia, S.S. (1996). Endoproteolysis of presenilin 1 and accumulation of processed derivatives in vivo. Neuron *17*, 181–190.

Van Nostrand, W.E., Wagner, S.L., Suzuki, M., Choi, B.H., Farrow, J.S., Geddes, J.W., Cotman, C.W., and Cunningham, D.D. (1989). Protease nexin-II, a potent antichymotrypsin, shows identity to amyloid β-protein precursor. Nature *341*, 546–549.

Wasco, W., Pettingell, W.P., Jondro, P.D., Schmidt, S.D., Gurubhagavatula, S., Rodes, L., DiBlasi, T., Romano, D.M., Guenette, S.Y., Kovacs, D.M., Growdon, J.H., and Tanzi, R.E. (1995). Familial Alzheimer's chromosome 14 mutations. Nature Med. *1*, 848.